



Comparison of seismic vulnerability analysis of steel-tube concrete arch bridges at different construction stages based on the probabilistic seismic demand analysis

Minhuan Liu^{a*}, Qianhua Yu^b

Changsha University of Technology, School of Civil Engineering, Changsha, 410114, China

^{a*}351424063@qq.com, ^b1594519760@qq.com

Abstract. In order to study the effects of earthquakes on the structure of large-span steel-tube concrete arch bridges under different construction states, a large-span steel-tube concrete arch bridge was selected as an actual construction case, and OpenSees was used to consider the internal forces during the actual construction process to establish a nonlinear dynamic analysis model for nine arch bridge construction phases, and 60 sets of typical impulse-type near-fault recordings were selected as inputs for ground shaking, and Probabilistic Seismic Demand Analysis was used to draw the seismic susceptibility curves of the bottom of the junction pier and the foot of the arch. The results show that: the bottom of the junction pier is less affected by the along-bridge ground vibration during the construction stage; the damage probability of the bottom of the junction pier after the closure is significantly reduced compared with that during the construction process before the closure; during the construction process, the transverse ground vibration has the greatest influence on the damage probability of the foot of the arch in terms of moderate damage, severe damage, and complete damage, which is second to that of the along-bridge ground vibration.

Keywords: steel-tube concrete arch bridge; construction process; probabilistic seismic demand analysis; seismic susceptibility curve.

1 Introduction

In recent decades, the construction of large-span steel-tube concrete arch bridges and construction technology has been rapidly developed over the years has made considerable achievements^[1]. For the bridge seismic vulnerability analysis mostly in the bridge stage, in the bridge construction, the bridge construction, between the components has not formed a complete structural system, the structural alignment and structural stress in the process of constant change, has not yet reached stability, the construction process of the displacement and stress and after the completion of the gap is large, the risk of seismic damage is also different^[2].

Bridge seismic vulnerability analysis for the probabilistic assessment of the seismic risk of highway bridges, which is essential for the pre-seismic planning and post-

seismic response of the transportation system^[3], in 1998, Shome N determines the ground shaking parameters by selecting recording samples with a given plot moment magnitude and the closest distance to the rupture zone, and obtains the engineering demand parameters through nonlinear response estimation, which are used to estimate the probability of the nonlinear structural response exceeding the given level, called the probabilistic seismic demand analysis. probability, called probabilistic seismic demand analysis^[4], and probabilistic seismic demand modeling^[5] can respond to the relationship between engineering demand parameters and ground shaking parameters, the accuracy of probabilistic seismic demand analysis relies on the uncertainty involved in probabilistic seismic demand modeling, and the accuracy depends on the selection of the ground shaking parameters.

In order to study the probability of seismic damage during the construction stage of steel-tube concrete arch bridges and to evaluate the seismic performance of steel-tube concrete arch bridges during the construction stage, this paper divides the construction case of diagonally-laying hook-and-loop cantilevered spandrel arch bridges into nine construction stages, and performs a nonlinear analysis of the structure with OpenSees under the stress conditions of each construction stage, taking into account the uncertainties of the seismic wave and the damage indexes, and selects a model for the construction of steel-tube concrete arch bridges from the Pacific Earthquake Engineering Research Center to select 60 ground shaking records, establish the probabilistic seismic demand model, plot the susceptibility curves of the bottom of the junction pier and the foot of the arch at each construction stage through the susceptibility function, and evaluate the probability of seismic risk of the bottom of the junction pier and the foot of the arch at each construction stage.

2 Construction process of steel pipe concrete arch bridge

In this paper, the actual construction project case of (35+260+35)m steel pipe concrete is used, which the whole bridge consists of diagonally tensioned buckled cantilever system and steel pipe concrete arch ribs as shown in Fig. 1. In order to study the seismic susceptibility analysis of the bottom of the junction pier and the foot of the arch bridge during the construction process, it will be divided into nine construction phases as shown in Table 1. The arch ribs, junction piers and buckling towers of OpenSees are modeled by nonlinear beam units, and the buckling anchorage cables are modeled by rod units, and the node mass is simulated by mass command.

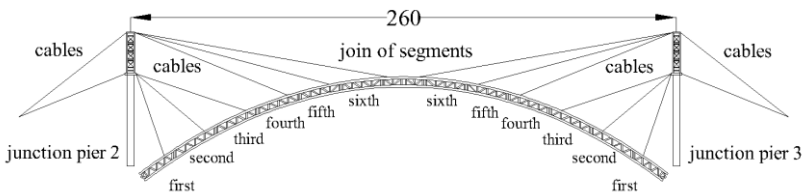


Fig. 1. Arch bridge cable-stayed fastening-hanging cantilever assembly plan

Table 1. Construction Stages of Arch Bridges

Construction Phase No.	Name of construction phase	Contents of construction
CS1	Lifting the first section	Junction pier buckling tower, articulated arch foot, first section of arch rib and tensioned first section of buckling anchor cable
CS2	Lifting the second section	Second section of arch ribs, installation and tensioning of second section of buckling anchors
CS3	Lifting the third section	Third section of arch ribs, installation and tensioning of third section of buckled anchors
CS4	Lifting of the fourth section	Fourth section of arch ribs, installation and tensioning of fourth section of buckling anchors
CS5	Lifting of the fifth section	Fifth section of arch ribs, installation and tensioning of fifth section of buckling anchors
CS6	Lifting of the sixth segment	Sixth section of arch ribs, installation and tensioning of sixth section of buckling anchors
CS7	Join of segments	Arch rib closing
CS8	Seal stranding and unbuttoning	Foot of arch stranding to solid joint, removal of buckling anchors and buckling towers
CS9	Pouring concrete for arch ribs	Pouring concrete for arch ribs

3 Seismic vulnerability analysis

In this paper, the type of seismic wave is selected as pulse velocity effect near-field earthquake, and $R=25\text{Km}$ is used as the demarcation between near-field and far-field earthquakes, 60 ground shaking records and two horizontal components of 2D seismic wave samples are selected from the Pacific Earthquake Engineering Research Center, and the combination of seismic wave inputs is classified into two types, i.e., longitudinal bridging and transverse bridging, and selecting the reasonable ground shaking parameter (IM) is an probabilistic seismic demand model important component, and the peak ground shaking acceleration (PGA) is adopted as the judgment standard of seismic intensity.

As shown in equation (1), the curvature ductility ratio of the intersection pier base section is used as the damage index (I_j), and the dual parameter damage model of the compression bending coefficient of the arch foot section and the accumulated energy of the section is used as the damage index (I_g)^[6], as shown in equation (2), where λ The bending coefficient, represented as the corresponding function of the P-M curve, is given in equation (2). In equation (2), N , M , N_u , and M_u correspond to the section axial force, bending moment, ultimate axial force, and ultimate bending moment, respectively. E_n represents strain energy. For nine construction stage models of steel-concrete arch bridges, each construction stage model inputs 60 transverse and 60 longitudinal

seismic motions to obtain the maximum damage index (I_j) of the bridge pier base under transverse seismic motion and the maximum damage index (I_j) of the bridge pier base under longitudinal seismic motion. The damage index (I_g) of the arch foot under transverse seismic motion is obtained The maximum value is 60 and the maximum damage index (I_g) of the arch foot under longitudinal seismic motion is 60. According to linear regression theory, the univariate linear equations of the logarithm of the damage index ($\ln(I)$) and the logarithm of the seismic motion parameters ($\ln(IM)$) are obtained. The model equation is shown in equation (3). The damage indicators and PGA linear equation diagram for each construction stage are shown in Figure 2.

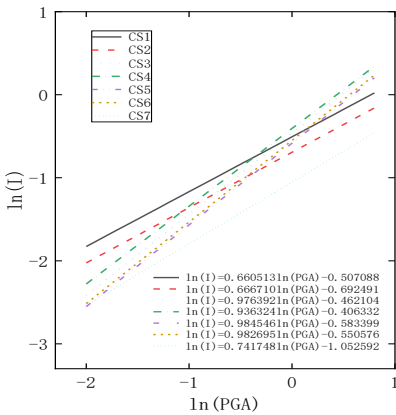
$$I_j = \frac{\phi}{\phi_y} \tag{1}$$

$$I_g = \frac{\lambda}{\lambda_u} + \beta \left(\frac{\int E_h dl}{\int (N_u \epsilon_u + aM_u \phi_u) dl} \right)$$

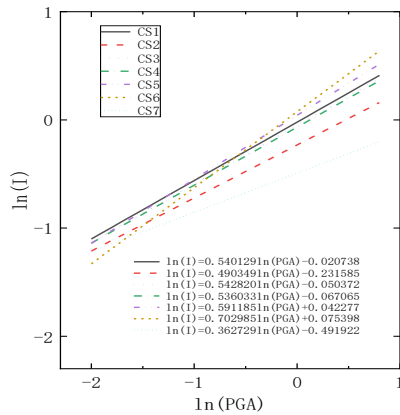
$$N/N_u \geq 2\eta_0, \lambda = \frac{N}{N_u} + a \frac{M}{M_u} \tag{2}$$

$$N/N_u < 2\eta_0, \lambda = -b \left(\frac{N}{N_u} \right)^2 - c \left(\frac{N}{N_u} \right) + \frac{M}{M_u}$$

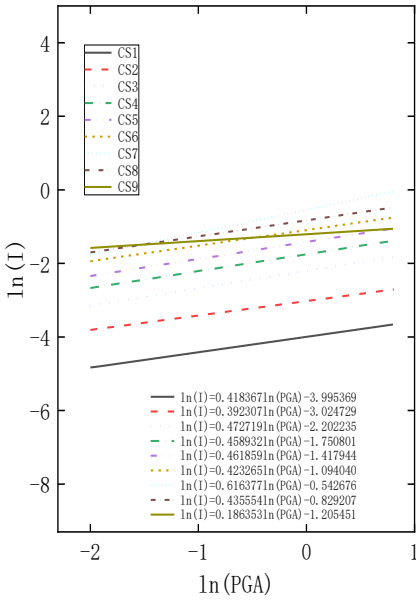
$$\ln(I) = \ln(a) + b\ln(IM) \tag{3}$$



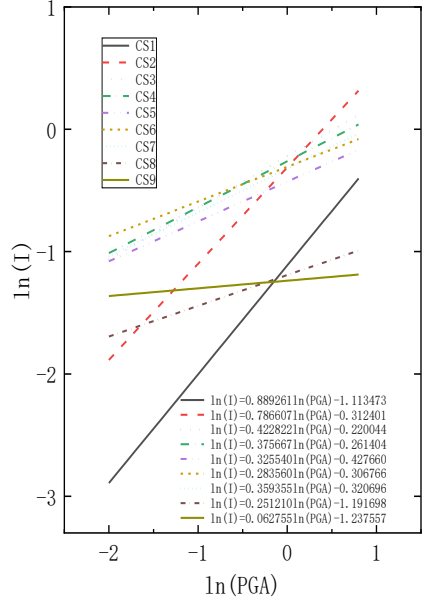
(a) Relationship between damage indicators and PGA at the bottom of junction piers under longitudinal bridge oriented ground shaking effects



(b) Relationship between damage indicators and PGA at the base of junction piers under transverse bridge oriented ground shaking effects



(c) Relationship between damage indexes and PGA of arch footing under longitudinal bridge oriented ground shaking effects



(d) Relationship between damage indexes and PGA of arch footing under transverse bridge oriented ground shaking effects

Fig. 2. Relationship between damage indicators and PGA

According to the seismic vulnerability curve function^[7], it can be expressed as equation (4), $\sqrt{\beta_{EDP|IM}^2 + \beta_c^2} = 0.5$, where the four failure levels d at the bottom of the junction pier are 1, 1.3, 4.7, 15.6; The four failure levels d of the arch foot are 0.1, 0.3, 0.5, and 0.7; According to equations (3) and (4), the vulnerability curve function can be used to calculate the vulnerability curve at the bottom of the junction pier, as shown in Figure 3, and the vulnerability curve at the arch foot is shown in Figure 4.

$$P_r(D \geq C | IM) = \Phi\left[\frac{\ln(I) - \ln(d)}{\sqrt{\beta_{EDP|IM}^2 + \beta_c^2}}\right] \quad (4)$$

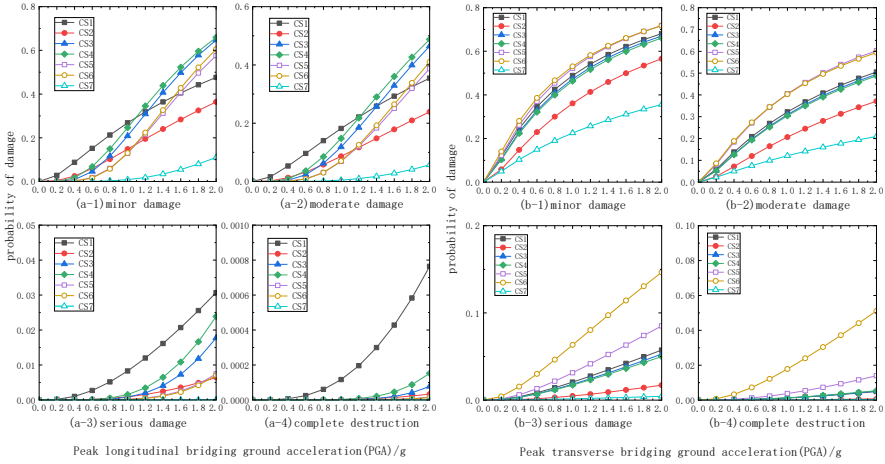


Fig. 3. Seismic vulnerability curves of the bottom of the junction pier

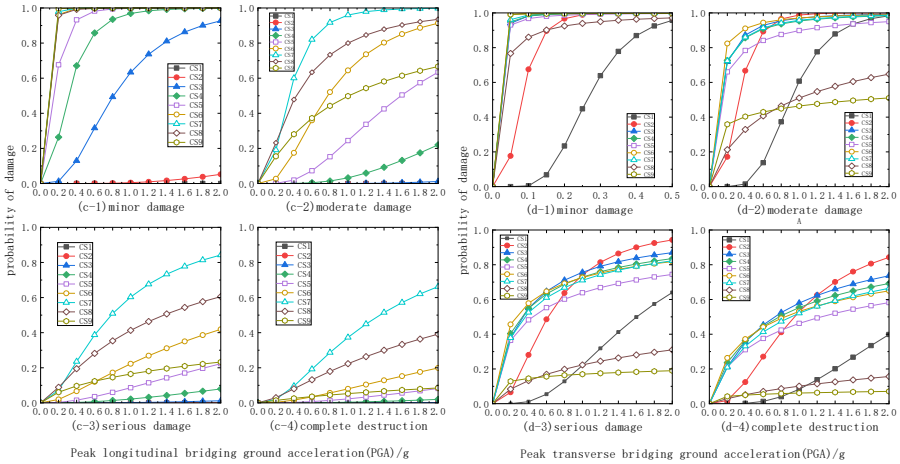


Fig. 4. Seismic vulnerability curve of arch footing

4 Conclusion

(1) At $PGA < 1g$, the probability of damage at the bottom of the junction pier in the construction stage of CS1 is the largest under the effect of ground vibration in the downward direction, and the probability of damage at the bottom of the junction pier in the construction stage of CS6 is the largest under the effect of ground vibration in the transverse direction in the whole bridge construction process.

(2) The damage probability of the bottom of the junction pier after the closure is significantly reduced compared with the damage probability in the construction process

before the closure, and the probability of serious damage and complete destruction is close to 0.

(3) The probability of damage to the arch foot increases with the advancement of the construction process of the cantilever assembly under the action of ground vibration in the direction of the bridge, and reaches the maximum at the time of closing, and the probability of damage decreases after the sealing strand is removed from the buckles, and decreases again after the pouring of concrete, and the damage to the arch foot has no influence on the ground vibration in the construction stage of the bridge in the direction of the bridge CS1~CS2, and the main influence comes from the action of ground vibration in the direction of the transverse bridge.

(4) Cross-bridge ground vibration in the construction process of the foot of the arch of moderate damage, serious damage, complete destruction of the damage probability of the impact is greater than along the bridge to the ground vibration.

Reference

1. Zheng J L, Wang J J. (2018) Concrete-Filled steel tube arch bridges in China. *J. Engineering*, 4(1): 143-155. DOI: 10.1016/j.eng.2017.12.003.
2. Xiong H Z, Jiang S T, Huang Y, Zhang J. (2022) Seismic vulnerability analysis of simply supported continuous bridge during construction. *J. Multidiscipline Modeling in Materials and Structures*, 18(3): 459-476. DOI:10.1108/MMMS-03-2022-0029.
3. Billah A H M M, Alam M S. (2015) Seismic fragility assessment of highway bridges: a state-of-the-art review. *J. Structure and Infrastructure Engineering*, 11(6): 804-832. DOI: 10.1080/15732479.2014.912243.
4. Shome N, Comell C A, Bazzurro P, Carballo J E. (1998) Earthquakes, records, and nonlinear responses. *J. Earthquake Spectra*, 14(3): 467-500. DOI: 10.1193/1.1586011.
5. Liu X L, SU C. (2020) Seismic fragility analysis of long-span bridges based on explicit time-domain method. *J. Journal of Vibration Engineering*, 33(4): 815-823. DOI: 10.16385/j.cnki.issn.1004-4523.2020.04.020.
6. Xie K Z, Lv W G, Tan L Q. (2012) Research on seismic damage evaluation of CFST arch bridges. *J. China Journal of Highway and Transport*, 25(2): 53-59. DOI: 10.19721/j.cnki.1001-7372.2012.02.008.
7. Pan H Y, Li T, Fu X. (2020) Sensitivities of the seismic response and fragility estimate of a transmission tower to structural and ground motion uncertainties. *J. Journal of Constructional Steel Research*, 2020, 167: 105941. DOI: 10.1142/S0219455423501961.

Open Access This chapter is licensed under the terms of the Creative Commons Attribution-NonCommercial 4.0 International License (<http://creativecommons.org/licenses/by-nc/4.0/>), which permits any noncommercial use, sharing, adaptation, distribution and reproduction in any medium or format, as long as you give appropriate credit to the original author(s) and the source, provide a link to the Creative Commons license and indicate if changes were made.

The images or other third party material in this chapter are included in the chapter's Creative Commons license, unless indicated otherwise in a credit line to the material. If material is not included in the chapter's Creative Commons license and your intended use is not permitted by statutory regulation or exceeds the permitted use, you will need to obtain permission directly from the copyright holder.

